DOI: 10.1534/genetics.107.070987

Note

A Role for *Caenorhabditis elegans* Chromatin-Associated Protein HIM-17 in the Proliferation *vs.* Meiotic Entry Decision

Jessica B. Bessler,*[,1] Kirthi C. Reddy,*[,1] Michiko Hayashi,* Jonathan Hodgkin[†] and Anne M. Villeneuve*[,2]

**Department of Developmental Biology and Department of Genetics, Stanford University School of Medicine, Stanford, California 94305 and [†]Genetics Unit, Department of Biochemistry, University of Oxford, Oxford OX1 3QU, United Kingdom*

Manuscript received November 27, 2006
Accepted for publication January 16, 2007

ABSTRACT

Chromatin-associated protein HIM-17 was previously shown to function in the chromosomal events of meiotic prophase. Here we report an additional role for HIM-17 in regulating the balance between germ cell proliferation and meiotic development. A cryptic function for HIM-17 in promoting meiotic entry and/or inhibiting proliferation was revealed by defects in germline organization in *him-17* mutants grown at high temperature (25°) and by a synthetic tumorous germline phenotype in *glp-1(ar202); him-17* mutants at 15°.

REPRODUCTIVE success in animals requires a confluence of events within the germline. To generate haploid gametes, germ cells must undergo a meiotic program involving a coordinated sequence of chromosome reorganization and remodeling events that culminate in the segregation of homologous chromosomes. These events include homolog pairing and synapsis, formation and repair of double-strand DNA breaks (DSBs) to generate crossovers, and maturation of crossovers into chiasmata. Further, these chromosomal events occur in parallel with gametogenesis programs that generate the highly specialized sperm and egg cells that will unite to form the zygote. Finally, since meiotic entry represents the onset of cellular differentiation, meiosis must be balanced with germ cell proliferation to ensure a sufficient supply of gametes.

Although gametogenesis, meiosis, and meiotic entry programs must ultimately be coordinated to accomplish successful reproduction, they operate largely independently of each other. *Caenorhabditis elegans* mutants that are profoundly defective in the chromosomal events of meiosis can undergo an otherwise normal gametogenesis (*e.g.*, Dernburg *et al.* 1998; MacQueen and Villeneuve 2001; MacQueen *et al.* 2002), and in mutants defective in regulating the spatial and temporal pattern of meiotic entry, the execution of meiosis and gametogenesis can be substantially normal despite occurring in an inappropriate context (Austin and Kimble 1987). Links between germline programs often involve regulatory couplings, such as checkpoints triggered by defects in synapsis or recombination (*e.g.*, Ghabrial *et al.* 1998; Bhalla and Dernburg 2005; Cohen *et al.* 2006), or reflect repeated use of the same molecular components (*e.g.*, Francis *et al.* 1995a,b; Hansen *et al.* 2004).

Here we report a convergence between two largely independent facets of sexual reproduction in *C. elegans*, the proliferation *vs.* meiosis entry switch and the chromosomal events of meiotic prophase, identified through analysis of *him-17* mutants. We first identified HIM-17 on the basis of its role in meiotic recombination (Reddy and Villeneuve 2004). HIM-17 is associated with chromatin throughout the germline and is a modular protein containing six repeats of a putative DNA-binding motif also found in several other proteins implicated in chromatin regulation through genetic interactions with LIN-35/Rb (Ferguson and Horvitz 1989; Clark *et al.* 1994; Thomas and Horvitz 1999; Chesney *et al.* 2006). Under standard conditions (20°), *him-17* mutants exhibit normal pairing and synapsis but have reduced or delayed DSB formation, leading to a deficit of crossovers and chiasmata. Chiasmata can be restored by radiation-induced DSBs, indicating that all other components needed to generate crossovers and chiasmata are present. HIM-17 is also required for proper accumulation of histone H3 dimethylation at lysine 9 (H3K9me2) on meiotic prophase chromosomes.

[1]These authors contributed equally to this work.

[2]*Corresponding author:* Department of Developmental Biology, Stanford University School of Medicine, 279 Campus Dr., Beckman Center B300, Stanford, CA 94305-5329. E-mail: villen@cmgm.stanford.edu

TABLE 1

Temperature-sensitive sterility of *him-17* mutants

Genotype	Mean no. of eggs/brood ± SD	
	20°	25°
Wild type	274 ± 26[a]	204 ± 15
him-17(e2707)	229 ± 30[a]	0.4 ± 1
him-17(me9)	220 ± 27[a]	0.3 ± 0.7
him-17(me24)	225 ± 27[a]	0
him-17(ok424)	227 ± 37[a]	0
spo-11(ok79)	222 ± 21	175 ± 23
chk-2(me64)	200 ± 15	197 ± 20

Ten complete broods were counted for each genotype at each temperature. Hermaphrodite worms were shifted to 25° at the L3 stage. *him-17* alleles are listed in order of decreasing *him-17* activity.

[a] Data are from Reddy and Villeneuve (2004).

This work reveals an additional role for HIM-17 in promoting meiotic entry and/or in inhibiting proliferation of germ cells. We show that *him-17* mutants exhibit defective germline patterning and sterility at 25° that cannot be explained as a consequence of the previously described defects in the chromosomal events of meiosis. Further, a synthetic tumorous germline phenotype in *glp-1(ar202); him-17* mutants at 15° indicates that reduced *him-17* function affects the efficacy of the GLP-1/Notch signaling pathway that serves as the master regulator of the mitosis/meiosis switch (Hansen and Schedl 2006).

***him-17* mutants exhibit temperature-sensitive sterility characterized by defects in germline organization:** *him-17* mutant worms grown at 15° or 20° usually display normal meiotic prophase progression, are competent to complete the meiotic program, and produce normal numbers of embryos, although chromosome missegregation renders many embryos inviable. At 25°, hermaphrodites with reduced *him-17* function are sterile, producing virtually no embryos (Table 1) or unfertilized oocytes. High-temperature sterility was observed for all five independently isolated *him-17* alleles and for *him-17*(RNAi) worms, indicating that there is a process that is vulnerable to loss of HIM-17 function only at high temperature.

Cytological analysis revealed defects in germline organization in *him-17* adult hermaphrodites shifted from 20° to 25° as L3 larvae (hereafter referred to as "*him-17* 25° hermaphrodites") (Figure 1; Table 2). In wild-type hermaphrodites, mitotic proliferation occurs in the distal-most (premeiotic) region of the germline, and nuclei enter meiotic prophase as they move proximally into the transition zone; nuclei progressing from the pachytene through diakinesis stages of meiotic prophase are found in progressively more proximal positions. This temporal/spatial organization was disrupted in the germlines of all *him-17* 25° hermaphrodites examined. DAPI staining (Figure 1A) revealed diakinesis-like nuclei surrounded by pachytene-like nuclei, indicating that the orderly arrangement of meiotic prophase substages was perturbed, and normal-looking oocytes were not observed.

Further, immunostaining revealed mitotically cycling nuclei interspersed with meiotic prophase nuclei in *him-17* 25° hermaphrodites. Meiosis-specific chromosomal protein HIM-3 (Zetka *et al.* 1999) served as a marker for meiotic entry; in wild-type germlines, HIM-3 antibody does not stain premeiotic nuclei but stains all meiotic prophase nuclei, beginning at the transition zone. In *him-17* 25° hermaphrodites, nuclei with premeiotic-like DAPI signals that lacked HIM-3 staining were interspersed with meiotic prophase nuclei throughout the gonad (Figure 1B; Table 2). Most germlines also had elevated numbers of premeiotic nuclei in the distal region, suggesting excessive proliferation (Table 2). A few rare individuals (<5%) had a second zone of mitotic proliferation in the proximal gonad (1/30 gonads in HIM-3 immunofluorescence experiments; also seen but not quantified in DAPI-only experiments) or had largely tumorous germlines with very few, if any, meiotic nuclei (data not shown). Finally, an antibody detecting histone H3 phosphorylated at serine 10 (H3S10p), which stains mitotic figures (Hendzel *et al.* 1997; Lieb *et al.* 1998), revealed ectopic mitoses in over half of *him-17* 25° germlines (Figure 1C; Table 2). Together these observations suggest a defect in the regulation of mitotic proliferation and entry into meiosis in *him-17* 25° hermaphrodites.

A small fraction of *him-17* 25° hermaphrodites also exhibited an apparent defect in the spermatogenesis-to-oogenesis switch. In wild-type hermaphrodites, each gonad arm produces sperm during late larval growth and then switches to oogenesis in adulthood. In 7% of *him-17* 25° adult hermaphrodites examined at 48 hr post L4, we observed gonad arms that were filled with sperm (Figure 1D; Table 2).

him-17 male worms shifted to 25° as L1 larvae ("*him-17* 25° males") exhibited defects similar to those seen in *him-17* 25° hermaphrodites, including excess nuclei with the appearance of mitotically cycling cells and altered spatial organization of meiotic prophase stages and meiotic divisions. In addition, *him-17* 25° males contained reduced numbers of sperm, and although they appeared to exhibit normal mating behavior, mating and sperm transfer assays (Shakes and Ward 1989; Stanfield and Villeneuve 2006) revealed that they did not transfer either sperm or sperm-activating seminal fluid components to hermaphrodites (data not shown.)

Recombination failure does not lead to high-temperature sterility: High-temperature sterility is not a consequence of failure to initiate meiotic recombination, as *spo-11* mutants, which lack the meiotic DSB-forming enzyme (Dernburg *et al.* 1998), and *chk-2* mutants, in which *spo-11*-dependent DSBs are reduced or eliminated

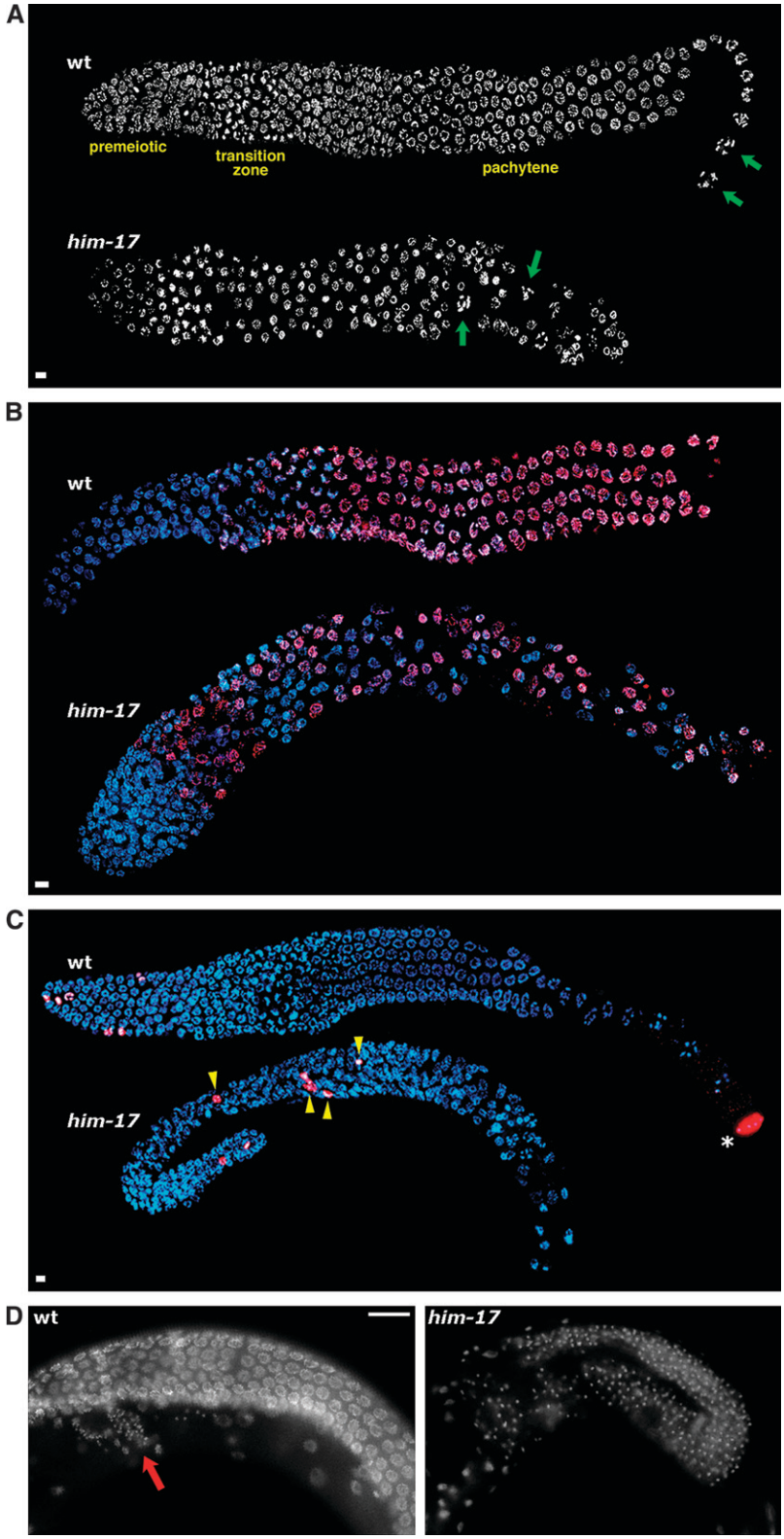

Figure 1.—*him-17* 25° hermaphrodites exhibit defects in germline organization. (A) DAPI-stained germlines of wild-type and *him-17(me24)* hermaphrodites raised at 25°. In the wild-type germline, nuclei at diakinesis, the last stage of meiotic prophase, are seen only in the most proximal region of the gonad (green arrows). These nuclei are characterized by highly compact chromosomes that are well separated from each other. In the *him-17* germline, diakinesis-like nuclei (green arrows) are seen in more distal regions interspersed with pachytene-like nuclei, indicating perturbed spatial organization of meiotic prophase substages. (B) Hermaphrodite germlines stained with HIM-3 antibody (red) and DAPI (blue). In the wild-type germline, HIM-3 antibody does not stain premeiotic nuclei but stains all meiotic prophase nuclei beginning in the transition zone. In the *him-17(ok424)* 25° germline, HIM-3-negative nuclei are seen throughout the gonad, interspersed with meiotic prophase nuclei. (C) Hermaphrodite germlines stained with H3S10p antibody (red) and DAPI (blue). In the wild-type germline, anti-H3S10p-stained mitotic figures are seen only in the distal tip of the gonad (left). The asterisk indicates a nucleus at the end of the diakinesis stage, which is also brightly stained with anti-H3S10; mitotic figures are easily distinguished from late diakinesis nuclei on the basis of the appearance of DAPI-stained chromatin. In the *him-17(me24)* 25° germline, mitotic figures are observed in ectopic positions (yellow arrowheads). (D) Images of whole-mount adult hermaphrodite worms stained with DAPI. The wild-type germline is undergoing oogenesis (oocyte nuclei are in a different focal plane); the small DAPI-stained foci in the region indicated by the red arrow correspond to the nuclei of sperm stored in the spermatheca. The *him-17(me24)* 25° gonad is filled with small DAPI foci corresponding to sperm nuclei, indicating a failure to switch from spermatogenesis to oogenesis. In A–D, worms were shifted to 25° at the L3 stage; upon reaching late L4, worms were selected for subsequent cytological analysis and maintained at 25° for 20–24 hr prior to fixation. For A–C, gonad dissection, fixation, staining, and imaging using the Deltavision deconvolution microscopy system were conducted as described (Reddy and Villeneuve 2004). Bars in A–C, 4 μm. Images are projections through 3D data stacks encompassing whole nuclei. Primary antibodies used were rabbit anti-HIM-3 (Zetka *et al.* 1999) and rabbit anti-H3S10p (Upstate 05-598). In D, whole worms were fixed with Carnoy fixative and stained with DAPI as described (Villeneuve 1994), and images were acquired using conventional fluorescence microscopy at a single focal plane. Bar in D, 20 μm.

(MacQueen and Villeneuve 2001; Alpi *et al.* 2003; Martinez-Perez and Villeneuve 2005), do not display any additional defects and produce normal numbers of embryos at 25° (Table 1). Similarly, we did not observe additional defects at 25° for *mre-11*, *syp-1*, *syp-2*, or *him-8* mutants (data not shown; Hodgkin *et al.* 1979; Chin and Villeneuve 2001; MacQueen *et al.* 2002; Colaiacovo *et al.* 2003).

Defective acquisition of H3K9me2 does not lead to high-temperature sterility: As *him-17* mutants have

TABLE 2

Penetrance of *him-17* high-temperature phenotypes

Genotype	Incidence of observed phenotype				
	Altered spatial organization[a]	Interspersed meiotic and mitotic nuclei[b]	Excess mitotic nuclei in distal germline[b]	Ectopic H3S10p-positive figures[c]	Mog phenotype[d]
him-17(e2707)	10/10				
him-17(me9)	26/26	14/14[e]	11/14		Observed but not quantified
him-17(me24)	50/50	9/9	7/9	15/26	5/72
him-17(ok424)	16/16	7/7	6/7		Observed but not quantified
him-17(RNAi)	16/16				

For experiments examining the effects of high temperature on *him-17* hermaphrodite germlines, *him-17(me24)* or *him-17(ok424)* m+z− homozygous mutant hermaphrodites (m, maternal contribution; z, zygotic contribution) were selected as non-Unc progeny of *him-17/nT1Unc* heterozygotes. For *him-17(me9)* or *him-17(e2707)*, m+z− homozygous mutant hermaphrodites were identified on the basis of their Him phenotype among the progeny of *him-17/+* mothers. Their m−z− progeny were shifted to 25° for subsequent analysis. *him-17* RNA interference was performed as in Reddy and Villeneuve (2004).

[a] Numbers are combined totals of worms stained with DAPI only and germlines stained with DAPI and either anti-HIM-3 or anti-H3S10p.

[b] Germlines were fixed and stained with DAPI and HIM-3 antibody; HIM-3-positive nuclei were scored as meiotic and HIM-3-negative nuclei were scored as mitotically cycling. In normal gonads, nuclei in the proximal half of the distal proliferative region are located adjacent to the gonad periphery, surrounding a central cytoplasmic core that is largely devoid of nuclei; in gonads that were scored as having excess mitotic nuclei in the distal proliferative region, the central core was instead filled with tightly packed HIM-3-negative nuclei.

[c] Germlines were fixed and stained with DAPI and H3S10p antibody. H3S10p-positive figures were scored as ectopic if they were located in positions outside of the normal proliferative zone (the distal-most 20 rows of nuclei).

[d] In gonads that were scored as Mog, there were no obvious signs of oocyte production and sperm nuclei were present in vast excess over the normal number, filling the proximal gonad and extending past the loop into the distal gonad (see Figure 1D). The Mog phenotype was also observed but not quantified in *him-17(me9)* and *him-17(ok424)* mutants.

[e] Of 14, 1 had a clear second zone of mitotic proliferation in the proximal arm of the gonad.

defective acquisition of the H3K9me2 chromatin mark on meiotic prophase chromosomes (Reddy and Villeneuve 2004), we tested other meiotic mutants for defects in H3K9me2 acquisition. Whereas *spo-11* (Reddy and Villeneuve 2004) and *mre-11* (data not shown) mutants exhibited normal H3K9me2, *chk-2* mutant hermaphrodite and male germlines displayed a reduction in H3K9me2 (Figure 2, A and B) similar to that seen in *him-17(ok424)*. In wild-type hermaphrodite germlines, H3K9me2 staining is first observed in the early-to-middle pachytene region and accumulates as nuclei progress through pachynema. In *chk-2* hermaphrodites, H3K9me2 staining was not observed until mid-to-late pachytene. Moreover, whereas the partnerless X chromosome in wild-type male germlines is heavily enriched for H3K9me2 staining (Kelly *et al.* 2002), this enrichment is absent in *chk-2* males. The fact that defective H3K9me2 acquisition is not accompanied by high-temperature sterility in *chk-2* mutants strongly suggests that reduced accumulation of H3K9me2 is not the cause of the temperature-sensitive sterility in *him-17* mutants.

***him-17* mutants do not display desilencing of a transgene array despite altered acquisition of H3K9me2:** High-temperature sterility coupled with the previously reported defect in H3K9me2 acquisition raised the possibility that global gene silencing mechanisms might be compromised in *him-17* mutants. Thus, we assessed whether impairment of *him-17* function would cause desilencing of repetitive transgene array *ccEx7271*. In wild-type worms, this array drives LET-858:GFP expression in somatic cells but is silenced in the germline (Kelly and Fire 1998); further, the silenced array is deficient in activation-associated histone modifications and is enriched for H3K9me2 (Kelly *et al.* 2002).

Although desilencing was observed in positive controls, no desilencing was seen in *him-17(ok424); ccEx7271* or *him-17(me24); ccEx7271* hermaphrodite or male germlines at either 20° or 25° (supplemental Table 1 at http://www.genetics.org/supplemental/), nor did we observe desilencing after propagating *him-17(me24); ccEx7271* hermaphrodites for several generations. H3K9me2 staining nevertheless indicated an altered histone modification state of the transgene array. Whereas germline nuclei in wild-type males carrying *ccEx7271* contained two domains of H3K9me2 staining corresponding to the X chromosome and the silenced array, in *him-17; ccEx7271* males we saw no bright domains of staining at either 20° or 25° (Figure 2C and data not shown), indicating that depletion of H3K9me2 is not sufficient to cause desilencing.

***glp-1(ar202gf); him-17* double mutants reveal a cryptic role for HIM-17 in promoting meiotic entry at low temperature:** As several aspects of the *him-17* 25° phenotype resemble phenotypes caused by elevated levels of

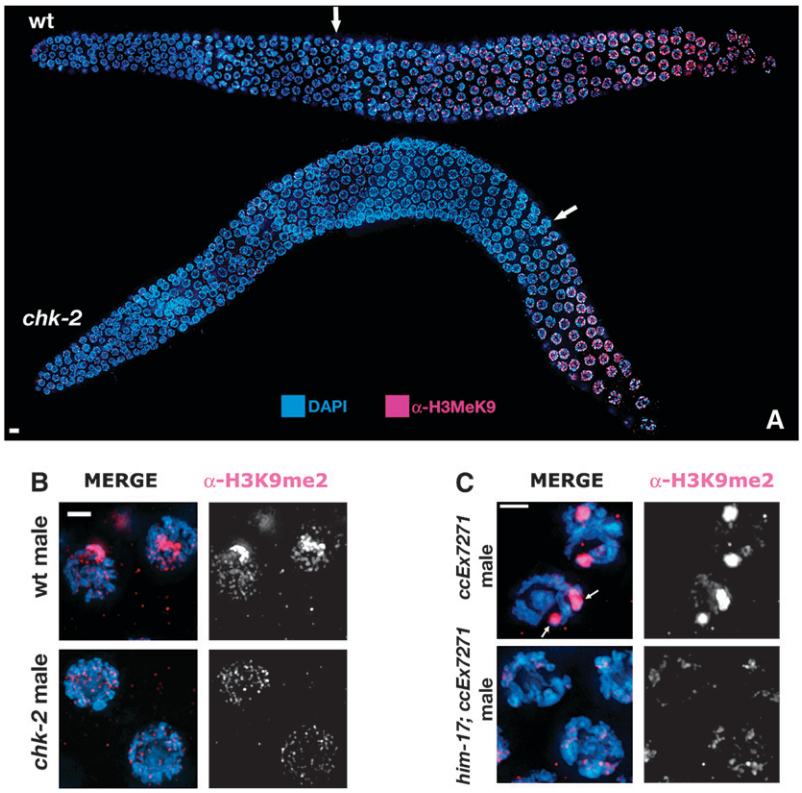

FIGURE 2.—H3K9me2 antibody staining of germline nuclei. (A and B) Altered H3K9me2 antibody staining in *chk-2* mutant germlines. DAPI-stained chromosomes are in blue; H3K9me2 is in red. (A) Low-magnification images of hermaphrodite germlines, oriented with the distal region to the left. In the wild-type germline, H3K9me2 is detected first as a single focus in nuclei in the early-to-middle pachytene region (arrow) and then in increasing amounts in nuclei in the late pachytene region. In the *chk-2(me64)* germline, staining appears much later in the pachytene region (arrow) and at substantially reduced levels. Bar, 4 μm. (B) High-magnification images of nuclei in the midpachytene region of XO male germlines. The brightly staining chromosome in the wild-type male corresponds to the partnerless X chromosome; this staining is greatly diminished in the *chk-2* male. Bar, 2 μm. (C) Altered H3K9me2 staining of a transgene array in *him-17* males. Midpachytene nuclei from wild-type and *him-17(me24)* males carrying extrachromosomal array *ccEx7271* and raised at 20°, stained with DAPI (blue) and anti-H3K9me2 (red). In each control male nucleus, there are two bright domains of H3K9me2 staining corresponding to the X chromosome and the transgene array (arrows). No bright domains of H3K9me2 staining are seen in the *him-17* male nuclei. Presence of the array in the pictured germlines was confirmed by demonstrating transmission of the array to progeny (see supplemental Table 1 at http://www.genetics.org/supplemental/) prior to fixation. Bar, 2 μm. In A–C, fixation, staining, and imaging were conducted as described (REDDY and VILLENEUVE 2004), and images are projections of 3D data stacks encompassing entire nuclei. The primary antibody was rabbit anti-H3K9me2 (Upstate 07-212).

GLP-1/Notch signaling, we investigated whether reduced *him-17* function could potentiate the elevated GLP-1 activity in weak *glp-1* gain-of-function mutants. Specifically, we tested whether *him-17* mutations could enhance the phenotype caused by *glp-1(ar202)*, a temperature-sensitive partial *glp-1* gain-of-function allele (PEPPER *et al.* 2003a); enhancement of *glp-1(ar202)* has been used previously as an indicator of defects in meiotic entry (HANSEN *et al.* 2004). *glp-1(ar202)* worms exhibit essentially normal germline patterning and fertility at 15° but show defective germline patterning at 25° characterized by ectopic and/or expanded zones of mitotic proliferation (PEPPER *et al.* 2003a). A prominent feature of *glp-1 (ar202)* 25° germlines is a zone of proliferating nuclei at the proximal end of the gonad (the Pro phenotype), proximal to a domain of meiotic nuclei; this phenotype appears to reflect a heightened response of the mutant GLP-1 protein to multiple anatomical sources of ligand (PEPPER *et al.* 2003b).

Whereas normal germline patterning was observed in all *glp-1(ar202)* or *him-17* single-mutant hermaphrodites at 15°, *glp-1(ar202); him-17* double-mutant hermaphrodites exhibited a highly penetrant tumorous germline phenotype at 15° for all four *him-17* alleles tested (Figures 3 and 4; Table 3; supplemental Figure 1 at http://www.genetics.org/supplemental/). By 48 hr post L4, affected worms exhibited massive germline tumors, with some gonads expanding to occupy nearly three times the normal space. These tumors appear similar to the synthetic germline tumors observed in *gld-2 gld-1* double mutants (HANSEN *et al.* 2004), as they contained some meiotic prophase nuclei and sperm interspersed between large zones of proliferating nuclei. *glp-1(ar202); him-17* males also exhibited tumorous germlines (Figure 3) with properties similar to those seen in hermaphrodites.

Time-course analysis at 15° using DAPI-stained whole-mount worms supports the conclusion that *glp-1(ar202); him-17* germline tumors result from a defect in meiotic entry (Figure 3A). Control *him-17(me9)* gonads exhibited normal organization along the proximal/distal axis at all time points examined. In L4 hermaphrodites, either spermatocytes (undergoing meiotic divisions) or haploid spermatids followed by spermatocytes were found at the proximal end of the gonad arm (adjacent to the spermatheca), followed by meiotic prophase nuclei and mitotically proliferating nuclei in progressively more distal positions. A similar organization was seen at 12 hr post L4, with many sperm having entered the spermatheca; by 24 hr post L4, spermatogenesis was complete and diakinesis-stage oocytes were found at the proximal end. Gonads of *glp-1(ar202)* single-mutant worms raised at 15° similarly exhibited normal spatial organization along the proximal/distal axis, although the onset of

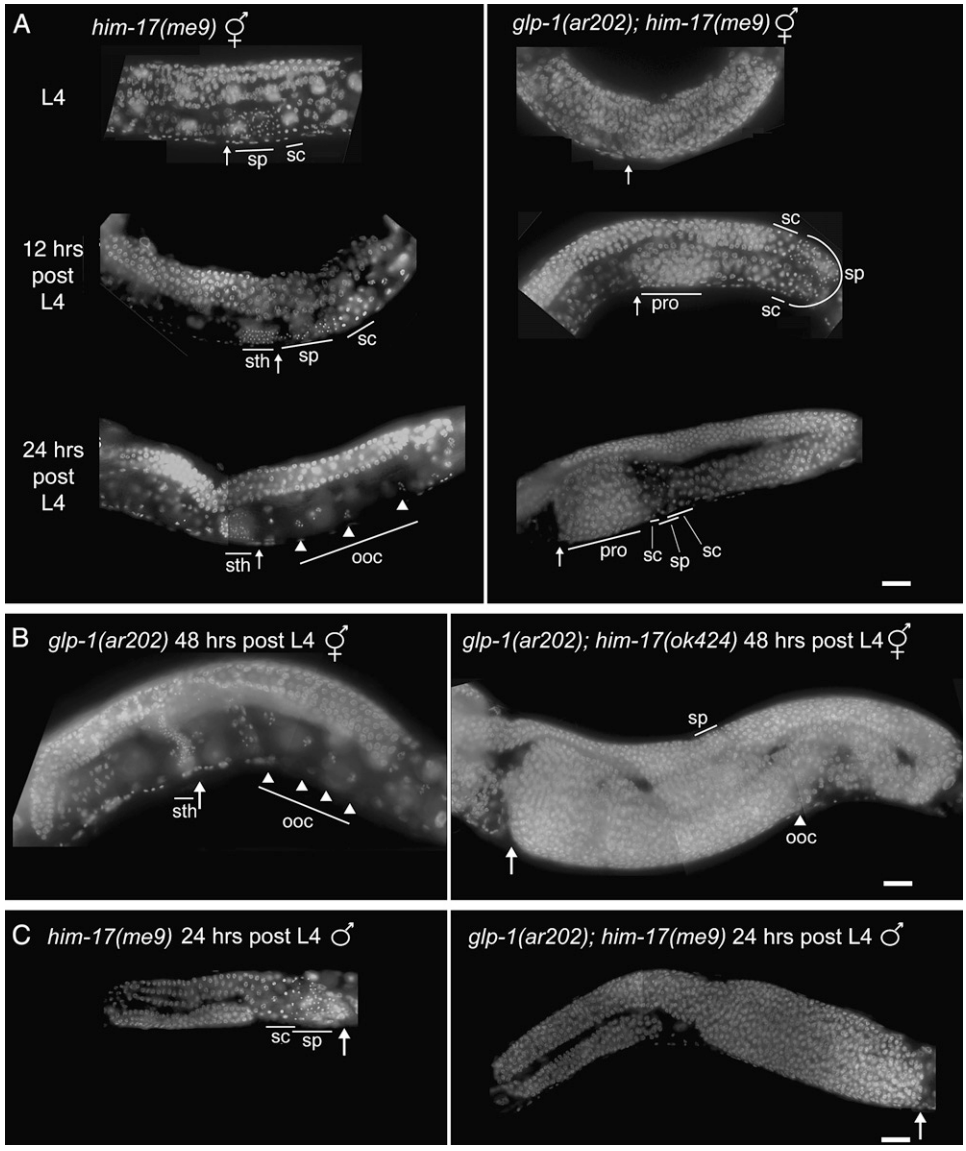

FIGURE 3.—Development of germline tumors at 15° in *glp-1 (ar202gf); him-17* double mutants. DAPI-stained gonads within whole-mount hermaphrodites (A and B) or males (C) fixed at the indicated time points. "sth" indicates sperm in the spermatheca; "sp" indicates sperm not in the spermatheca; "sc" are primary and secondary spermatocytes; "ooc" and arrowheads indicate oocytes; arrows point to the proximal end of the germline; "pro" indicates the location of proximal overproliferation. (A) (Left) Single-mutant *him-17(me9)* hermaphrodites fixed at L4, 12 hr post L4, and 24 hr post L4. (Right) *glp-1 (ar202); him-17(me9)* hermaphrodites at the same time points. *him-17(me9)* worms exhibit proper gonad organization at all time points. The L4 worm exhibits sperm and spermatocytes at the leading edge of the germline; by 12 hr post L4, some of the sperm have made it into the spermatheca, and at 24 hr post L4, all sperm are in the spermatheca, spermatocytes are no longer visible, and oocytes have developed. *glp-1(ar202); him-17(me9)* worms exhibit defects at all time points, including a delay in the appearance of spermatocytes and sperm, improper placement of spermatocytes and sperm once they are produced, and zones of ectopic proliferation. (B) (Left) *glp-1(ar202)* single-mutant hermaphrodite fixed at 48 hr post L4, exhibiting normal germline organization. (Right) *glp-1(ar202); him-17(ok424)* hermaphrodite at the same time point, exhibiting a massively overproliferated germline. (C) *him-17(me9)* and *glp-1(ar202); him-17(me9)* XO males at 24 hr post L4. In A–C, whole worms were fixed with ethanol and stained on slides with DAPI in a procedure modified from PEPPER *et al.* (2003a). Worms were picked directly into a minimal volume of M9 on a microscope slide and excess liquid was wicked away. Whole worms were fixed by adding 15 μl of 95% ethanol. Once dry, ethanol was added to the worms twice more. A 1:1 mixture of DAPI:Vectashield (Vector Laboratories, Burlingame, CA) was then added to the worms and the slides were sealed. Slides were stored up to 4 days at 4° before analysis with a standard fluorescence microscope with a CCD camera. Bars, 20 μm.

meiosis was temporally delayed. None of the *glp-1(ar202)* worms examined at late L4 or 6 hr post L4 contained detectable sperm, and only 1 of 12 had visible spermatocytes; however, sperm and spermatocytes were detected at the normal position in 6/6 worms at 12 hr post L4. [A delay in initial meiotic entry at 25° was previously reported for *glp-1(ar202)* (PEPPER *et al.* 2003b).]

Gonads from *glp-1(ar202); him-17(me9)* hermaphrodites exhibited differences from one or both single mutants at 15° at all time points examined. As in *glp-1(ar202)* worms, neither sperm nor spermatocytes were evident either at late L4 or 6 hr post L4, indicating a delay in meiotic entry. Moreover, when sperm and spermatocytes were first detected in *glp-1(ar202); him-17(me9)* gonads at 12 hr post L4, they were not located at the proximal end of the gonad but were instead found in much more distal positions, flanked both proximally and distally by spermatocytes undergoing meiotic divisions and nuclei in meiotic prophase, apparently indicative of a duplicated axis of meiotic entry and progression. Further, the most proximal ends of the germlines contained abundant nuclei with the size and appearance of proliferating germ cell nuclei, representing the early stages of a Pro tumor. By 24 hr post L4, these Pro tumors had expanded substantially, and overproliferation was also evident in the distal gonad.

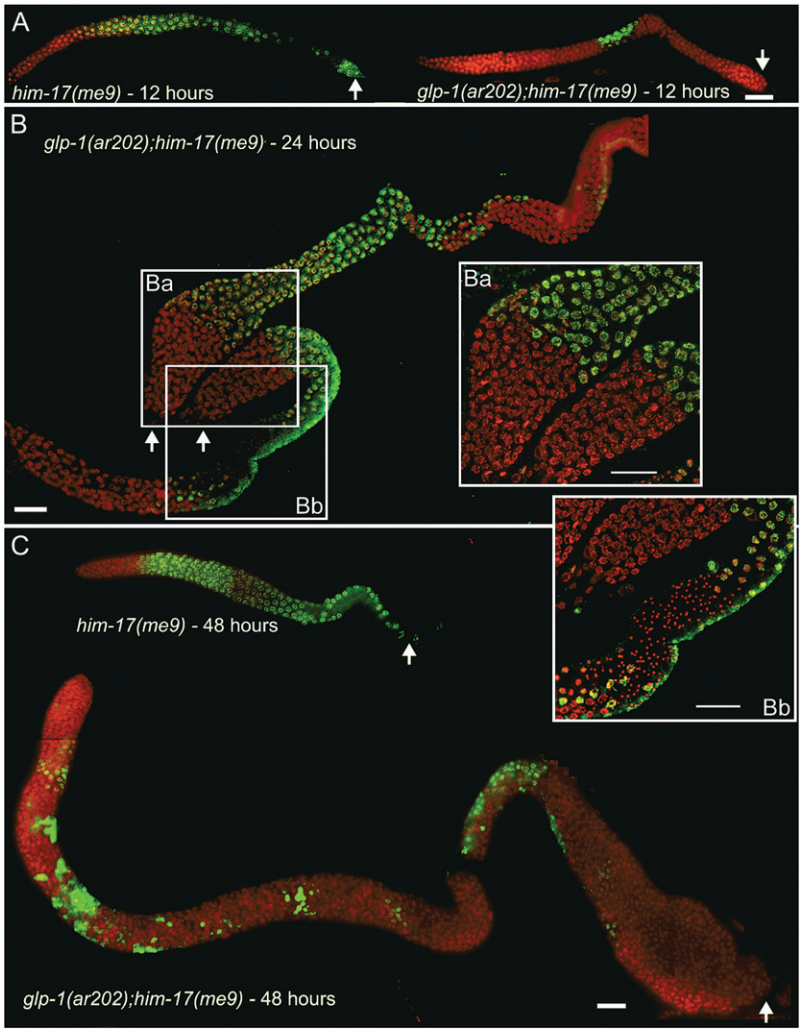

FIGURE 4.—Immunofluoresence analysis of developing tumorous germlines. Dissected gonads from *him-17(me9)* and *glp-1(ar202); him-17(me9)* hermaphrodites processed for immunofluoresence at the indicated time points. Staining with HIM-3 antibody (green) indicates meiotic nuclei; mitotically proliferating nuclei are stained with DAPI (red) only. In postmeiotic sperm, HIM-3 is retained in the cytoplasm but is no longer associated with the chromatin. Arrows indicate the proximal end of the germline. (A) 12 hr post L4. The *him-17(me9)* control shows a wild-type HIM-3-staining pattern, with HIM-3-positive meiotic nuclei extending from the transition zone to the proximal end of the gonad. The *glp-1(ar202); him-17(me9)* gonad exhibits HIM-3-positive meiotic nuclei only at a medial position, flanked by proliferating nuclei both proximally and distally; further, the distal mitotic region is extended compared to the *him-17(me9)* control. (B) 24 hr post L4. Two *glp-1(ar202); him-17(me9)* gonad arms from the same worm, both exhibiting large proximal tumors. Inset Ba highlights the two proximal tumors, one from each gonad arm; both are composed of a large region of HIM-3-negative proliferating nuclei (red) adjacent to a zone of meiotic prophase nuclei (green). Inset Bb highlights the duplicated axis of meiotic entry. Adjacent to the proximal tumor, a zone of meiotic entry is apparent (green), with nuclei progressing from meiotic prophase through spermatogenesis in a proximal-to-distal direction. In addition, meiotic entry has also occurred in the normal distal-to-proximal orientation (bottom), such that the two domains of meiotic progression converge on a single zone of haploid sperm. (C) 48 hr post L4. The *him-17(me9)* gonad exhibits the wild-type HIM-3-staining pattern, whereas the *glp-1(ar202); him-17(me9)* gonad is extensively overproliferated and contains mostly mitotically proliferating nuclei interspersed with small groups of HIM-3-positive meiotic nuclei. In A–C, dissected gonads were fixed and stained as described (MACQUEEN and VILLENEUVE 2001) except antibody incubations were performed at room temperature; images in Ba and Bb were acquired and processed using the Deltavision microscopy system, while the images in the remaining panels were acquired using a conventional fluorescence microscope with a CCD camera. Bars, 20 μm.

Immunostaining of dissected gonads corroborated the above observations (Figure 4). At 12 hr post L4, HIM-3 staining in *glp-1(ar202); him-17(me9)* gonads was limited to a small zone of nuclei in a medial position, flanked both proximally and distally by large zones of nuclei lacking HIM-3, substantiating the conclusion that the earliest appearance of meiotic nuclei is both temporally delayed and ectopically positioned. Further, Figure 4B illustrates both robust proximal tumors and a clear duplicated axis of meiotic entry and progression, with sperm at the center of a meiotic domain flanked by two distinct proliferative zones. This organization has also been observed in *glp-1(ar202)* 25° germlines (PEPPER *et al.* 2003a; E. J. HUBBARD, personal communication) and in *lin-12(lf)* mutants in which proximal proliferation results from excess availability of uterine-derived LAG-2 (SEYDOUX *et al.* 1990) and is interpreted to reflect a distance-dependent escape of germline nuclei from the influence of proximal sources of GLP-1 ligand(s). Thus our data support the interpretation that the Pro phenotype in *glp-1(ar202); him-17* mutants results from proliferation of germ cells that failed to enter meiosis rather than from germ cells that entered meiosis but reverted to mitotic cycling.

Together, our results indicate that *glp-1(ar202); him-17* germline tumors result from an impaired ability to exit the mitotic cell cycle and enter meiosis in a temporally and spatially appropriate manner. Further, these results imply a role for HIM-17 in inhibiting proliferation and/or promoting meiotic entry.

The *glp-1(ar202); him-17* synthetic tumorous phenotype suggests that *him-17* mutations cause either increased susceptibility to, or elevated levels of, signaling through the GLP-1 pathway. This could reflect either a heightened responsiveness of germ cells or an increased supply and/or ectopic source(s) of GLP-1 ligand. Enhancement of *glp-1* activity by *him-17* mutations is unlikely to be caused by ectopic expression of *lag-2*, as we did not detect any

TABLE 3

Penetrance of germline tumors at 15°

Genotype (m−z−)[b]	No. of tumorous gonad arms/total[a]							
	L4	6 hr	12 hr	24 hr	48 hr	72 hr	96 hr	120 hr[c]
glp-1(ar202)	0/20	0/18	0/11	0/26	0/14	0/24	0/24	0/26
him-17(e2707)	—	—	—	0/20	0/18	0/28	0/18	0/20
him-17(me9)	0/11	0/8	0/16	0/36	0/35	—	—	—
him-17(me24)	—	—	—	—	0/22	—	—	—
him-17(ok424)	—	—	—	—	0/10	—	—	—
glp-1(ar202); him-17(e2707)	—	—	—	7/12	12/38	17/56	17/35	13/22
glp-1(ar202); him-17(me9)	8/8	6/6	14/14	17/17	27/27	—	—	—
glp-1(ar202); him-17(me24)	—	—	—	—	11/12	—	—	—
glp-1(ar202); him-17(ok424)	—	—	—	—	10/10	—	—	—

glp-1(ar202); him-17 double mutants were constructed at 15° by crossing *him-17* males with *unc-32(e189) glp-1(ar202)* hermaphrodites, allowing F_1 hermaphrodites to self-fertilize and plating individual F_2 Unc hermaphrodites. *unc-32 glp-1(ar202); him-17* homozygous F_2 hermaphrodites were identified on the basis of their Him phenotype, and the germlines of their offspring were examined by fluorescence microscopy following either DAPI staining of whole worms or immunostaining of dissected gonads. All analyses of double mutants and controls were performed at 15°. The images in Figures 3 and 4, supplemental Figure 1 (http://www.genetics.org/supplemental/), and the data in this table correspond to gonads from homozygous *glp-1(ar202); him-17* hermaphrodites derived from homozygous mutant mothers (referred to as m−z−). However, tumors were also observed in m+z− *glp-1(ar202); him-17* hermaphrodites (on the basis of appearance in the dissecting microscope). The penetrance and expressivity of the tumorous germline phenotype varied for the different *him-17* alleles, correlating roughly with the allele strength deduced from the severity of the meiotic phenotypes of the corresponding single mutants at 20° (Reddy and Villeneuve 2004). For *e2707* and *me9*, the mating schemes used to derive the *glp-1(ar202); him-17* genotypes yielded F_2 worms that could be verified as Him at the expected frequency (13/60 for *e2707*, 133/497 for *me9*), as these *m+z−* hermaphrodites were able to lay eggs and to produce progeny despite the fact that most (8/12 for *e2707* and 91/119 for *me9*) developed germline tumors visible by dissecting microscope. In contrast, fertile *glp-1(ar202); him-17(me24)* or *glp-1(ar202); him-17(ok424)* m+z− hermaphrodites whose genotypes could be verified by progeny testing were underrepresented among F_2 progeny in the construction scheme (12/140 for *me24*, 15/156 for *ok424*). This deficit was offset by a class of F_2 worms were either completely sterile or produced a few dead embryos but no viable offspring (most with obvious germline tumors visible by dissecting microscope); PCR genotyping indicated that most, if not all, of these worms also represented *glp-1(ar202); him-17(me24)* or *glp-1(ar202); him-17(ok424)* m+z− hermaphrodites.

[a] Numbers include data from both ethanol-fixed whole worms and formaldehyde-fixed dissected worms. For each worm examined, either one or both of the gonad arms were scored.

[b] All genotypes include the marker *unc-32(e189)*.

[c] Hours indicate the number of hours post L4 at which the gonads were fixed.

ectopic expression of a *lag2::gfp* reporter (Fitzgerald and Greenwald 1995) in the *him-17(me9)* background (data not shown). This result is consistent with HIM-17 acting within the germline to modulate the response to GLP-1 signaling. Further, several additional findings support the idea that HIM-17 may promote meiotic entry via effects on chromatin within germline nuclei: (1) HIM-17 shares a putative DNA-binding motif with four other *C. elegans* proteins implicated in chromatin regulation; (2) *him-17* exhibits germline-enriched expression (Reinke *et al.* 2000); and (3) HIM-17 is associated with chromatin in germ cell nuclei. However, LAG-2 is not the sole GLP-1/Notch ligand in *C. elegans*, and there is evidence for both *glp-1*-dependent and *glp-1*-independent influences of somatic gonad sheath cells in promoting germ cell proliferation (McCarter *et al.* 1997; Killian and Hubbard 2004, 2005). Thus it is also possible that HIM-17 might exert its effects by acting in the soma and/or in parallel with GLP-1 signaling.

Concluding remarks: Although HIM-17 is not strictly essential for regulation of meiotic entry, the disruption of germline organization in *him-17* mutants at 25° and the tumorous germline phenotype of *glp-1(ar202); him-17* worms at 15° reveal a vulnerability of this process to environmental and genetic variation in the absence of HIM-17. We suggest a role for HIM-17 in buffering the mitosis/meiosis switch against environmental fluctuation, ensuring that germ cells respond appropriately to the activation state of GLP-1 and other developmental cues under a variety of conditions. We favor the idea that HIM-17 impinges on the proliferation *vs.* meiotic entry decision through effects on the chromatin environment within germ cells.

We thank Jane Hubbard and Tim Schedl for helpful discussions, Sarah Wignall and Mara Schvarzstein for critical reading of the manuscript, the Caenorhabditis Genetics Center and the *C. elegans* Gene Knockout Consortium for strains, and M. Zetka for the HIM-3 antibody. This work was supported by a postdoctoral grant from the Susan G. Komen Breast Cancer Foundation to J.B.B. and by National Institutes of Health grant R01GM67268 to A.M.V.

LITERATURE CITED

Alpi, A., P. Pasierbek, A. Gartner and J. Loidl, 2003 Genetic and cytological characterization of the recombination protein RAD-51 in *Caenorhabditis elegans*. Chromosoma **112:** 6–16.

Austin, J., and J. Kimble, 1987 glp-1 is required in the germ line for regulation of the decision between mitosis and meiosis in *C. elegans*. Cell **51:** 589–599.

Bhalla, N., and A. F. Dernburg, 2005 A conserved checkpoint monitors meiotic chromosome synapsis in *Caenorhabditis elegans*. Science **310:** 1683–1686.

Chesney, M. A., A. R. Kidd, III and J. Kimble, 2006 *gon-14* functions with class B and class C synthetic multivulva genes to control larval growth in *Caenorhabditis elegans*. Genetics **172:** 915–928.

Chin, G. M., and A. M. Villeneuve, 2001 *C. elegans* mre-11 is required for meiotic recombination and DNA repair but is dispensable for the meiotic G(2) DNA damage checkpoint. Genes Dev. **15:** 522–534.

Clark, S. G., X. Lu and H. R. Horvitz, 1994 The *Caenorhabditis elegans* locus lin-15, a negative regulator of a tyrosine kinase signaling pathway, encodes two different proteins. Genetics **137:** 987–997.

Cohen, P. E., S. E. Pollack and J. W. Pollard, 2006 Genetic analysis of chromosome pairing, recombination, and cell cycle control during first meiotic prophase in mammals. Endocr. Rev. **27:** 398–426.

Colaiacovo, M. P., A. J. MacQueen, E. Martinez-Perez, K. McDonald, A. Adamo *et al.*, 2003 Synaptonemal complex assembly in *C. elegans* is dispensable for loading strand-exchange proteins but critical for proper completion of recombination. Dev. Cell **5:** 463–474.

Dernburg, A. F., K. McDonald, G. Moulder, R. Barstead, M. Dresser *et al.*, 1998 Meiotic recombination in *C. elegans* initiates by a conserved mechanism and is dispensable for homologous chromosome synapsis. Cell **94:** 387–398.

Ferguson, E. L., and H. R. Horvitz, 1989 The multivulva phenotype of certain *Caenorhabditis elegans* mutants results from defects in two functionally redundant pathways. Genetics **123:** 109–121.

Fitzgerald, K., and I. Greenwald, 1995 Interchangeability of *Caenorhabditis elegans* DSL proteins and intrinsic signalling activity of their extracellular domains in vivo. Development **121:** 4275–4282.

Francis, R., M. K. Barton, J. Kimble and T. Schedl, 1995a *gld-1*, a tumor suppressor gene required for oocyte development in *Caenorhabditis elegans*. Genetics **139:** 579–606.

Francis, R., E. Maine and T. Schedl, 1995b Analysis of the multiple roles of *gld-1* in germline development: interactions with the sex determination cascade and the glp-1 signaling pathway. Genetics **139:** 607–630.

Ghabrial, A., R. P. Ray and T. Schupbach, 1998 okra and spindle-B encode components of the RAD52 DNA repair pathway and affect meiosis and patterning in Drosophila oogenesis. Genes Dev. **12:** 2711–2723.

Hansen, D., and T. Schedl, 2006 The regulatory network controlling the proliferation-meiotic entry decision in the *Caenorhabditis elegans* germ line. Curr. Top. Dev. Biol. **76:** 185–215.

Hansen, D., E. J. Hubbard and T. Schedl, 2004 Multi-pathway control of the proliferation versus meiotic development decision in the *Caenorhabditis elegans* germline. Dev Biol **268:** 342–357.

Hendzel, M. J., Y. Wei, M. A. Mancini, A. Van Hooser, T. Ranalli *et al.*, 1997 Mitosis-specific phosphorylation of histone H3 initiates primarily within pericentromeric heterochromatin during G2 and spreads in an ordered fashion coincident with mitotic chromosome condensation. Chromosoma **106:** 348–360.

Hodgkin, J., H. R. Horvitz and S. Brenner, 1979 Nondisjunction mutants of the nematode *Caenorhabditis elegans*. Genetics **91:** 67–94.

Kelly, W. G., and A. Fire, 1998 Chromatin silencing and the maintenance of a functional germline in *Caenorhabditis elegans*. Development **125:** 2451–2456.

Kelly, W. G., C. E. Schaner, A. F. Dernburg, M. H. Lee, S. K. Kim *et al.*, 2002 X-chromosome silencing in the germline of *C. elegans*. Development **129:** 479–492.

Killian, D. J., and E. J. Hubbard, 2004 *C. elegans* pro-1 activity is required for soma/germline interactions that influence proliferation and differentiation in the germ line. Development **131:** 1267–1278.

Killian, D. J., and E. J. Hubbard, 2005 *Caenorhabditis elegans* germline patterning requires coordinated development of the somatic gonadal sheath and the germ line. Dev. Biol. **279:** 322–335.

Lieb, J. D., M. R. Albrecht, P. T. Chuang and B. J. Meyer, 1998 MIX-1: an essential component of the *C. elegans* mitotic machinery executes X chromosome dosage compensation. Cell **92:** 265–277.

MacQueen, A. J., and A. M. Villeneuve, 2001 Nuclear reorganization and homologous chromosome pairing during meiotic prophase require C. elegans chk-2. Genes Dev. **15:** 1674–1687.

MacQueen, A. J., M. P. Colaiacovo, K. McDonald and A. M. Villeneuve, 2002 Synapsis-dependent and -independent mechanisms stabilize homolog pairing during meiotic prophase in *C. elegans*. Genes Dev. **16:** 2428–2442.

Martinez-Perez, E., and A. M. Villeneuve, 2005 HTP-1-dependent constraints coordinate homolog pairing and synapsis and promote chiasma formation during *C. elegans* meiosis. Genes Dev. **19:** 2727–2743.

McCarter, J., B. Bartlett, T. Dang and T. Schedl, 1997 Soma-germ cell interactions in *Caenorhabditis elegans*: multiple events of hermaphrodite germline development require the somatic sheath and spermathecal lineages. Dev. Biol. **181:** 121–143.

Pepper, A. S., D. J. Killian and E. J. Hubbard, 2003a Genetic analysis of *Caenorhabditis elegans glp-1* mutants suggests receptor interaction or competition. Genetics **163:** 115–132.

Pepper, A. S., T. W. Lo, D. J. Killian, D. H. Hall and E. J. Hubbard, 2003b The establishment of *Caenorhabditis elegans* germline pattern is controlled by overlapping proximal and distal somatic gonad signals. Dev. Biol. **259:** 336–350.

Reddy, K. C., and A. M. Villeneuve, 2004 *C. elegans* HIM-17 links chromatin modification and competence for initiation of meiotic recombination. Cell **118:** 439–452.

Reinke, V., H. E. Smith, J. Nance, J. Wang, C. Van Doren *et al.*, 2000 A global profile of germline gene expression in *C. elegans*. Mol. Cell **6:** 605–616.

Seydoux, G., T. Schedl and I. Greenwald, 1990 Cell-cell interactions prevent a potential inductive interaction between soma and germline in *C. elegans*. Cell **61:** 939–951.

Shakes, D. C., and S. Ward, 1989 Initiation of spermiogenesis in *C. elegans*: a pharmacological and genetic analysis. Dev. Biol. **134:** 189–200.

Stanfield, G. M., and A. M. Villeneuve, 2006 Regulation of sperm activation by SWM-1 is required for reproductive success of *C. elegans* males. Curr. Biol. **16:** 252–263.

Thomas, J. H., and H. R. Horvitz, 1999 The *C. elegans* gene lin-36 acts cell autonomously in the lin-35 Rb pathway. Development **126:** 3449–3459.

Villeneuve, A. M., 1994 A *cis*-acting locus that promotes crossing over between X chromosomes in *Caenorhabditis elegans*. Genetics **136:** 887–902.

Zetka, M. C., I. Kawasaki, S. Strome and F. Muller, 1999 Synapsis and chiasma formation in *Caenorhabditis elegans* require HIM-3, a meiotic chromosome core component that functions in chromosome segregation. Genes Dev. **13:** 2258–2270.

Communicating editor: B. J. Meyer